17th World Conference on Earthquake Engineering, 17WCEE
Sendai, Japan - September 13th to 18th 2020

ANALYSIS OF EARTHQUAKE-TRIGGERED LANDSLIDES WITH A GENERALIZATION OF THE NEWMARK METHOD

S. Dong[(1)], A. Ledesma[(2)], F. López-Almansa[(3)], W. Feng[(4)]

[(1)]*State Key Laboratory of Geohazard Prevention and Geoenvironment Protection (Chengdu University of Technology), Chengdu, dongshan1994@hotmail.com*
[(2)]*Professor, Technical University of Catalonia, Civil and Environmental Eng. Department, Barcelona, alberto.ledesma@upc.edu*
[(3)]*Professor, Technical University of Catalonia, Architecture Technology Department, Barcelona, francesc.lopez-almansa@upc.edu; currently Associate Researcher Natural and Anthropogenic Risks Research Center, Univ. Austral de Chile, Valdivia*
[(4)]*State Key Laboratory of Geohazard Prevention and Geoenvironment Protection (Chengdu University of Technology), Chengdu, fengwenkai@cdut.cn*

Abstract

Earthquake-triggered landslide is a highly serious issue, having caused important damages and considerable fatalities worldwide. The most popular software codes in geotechnical earthquake engineering (e.g. PLAXIS) experience big difficulties in reproducing this issue, mostly because do not consider large strains; they are necessary to reproduce the huge relative displacements involved in sliding. Other requirements prevent the use of such simulation tools: the boundary conditions need to incorporate some flexibility to describe the absorbing behavior, and the complexity of the nonlinear soil behavior during sliding must be characterized with many parameters, among other considerations. Conversely, the Newmark method was proposed long ago, and has been widely used, mainly because of its simplicity and reliability. However, the Newmark method involves important simplifications and has not been calibrated with time-history analyses, experimental results, or observed slides; thus, a number of improvements and generalizations have been reported so far. Inside this context, this work proposes a general approach that overcomes most of the limitations and weaknesses of the previous models but still provides a rather simple algorithm. The presented formulation considers the soil flexibility, accounts for the influence of the pore water pressure, and includes sliding criteria for both drained and undrained situations. Application examples of the proposed algorithm are presented: (i) sliding of a rigid block on a flat surface, (ii) comparison between the classical Newmark approach, (iii) influence of water pressure, (iv) influence of the soil flexibility, and (v) influence of the soil damping.

This work is a part of a broader research activity on seismic stability of soil slopes; includes deriving simple but accurate numerical models of earthquake-triggered landslides, conducting parametric studies, and performing laboratory experiments.

Keywords: Earthquake-triggered landslides; Newmark method; soil nonlinear time-history analysis; Sliding displacement.

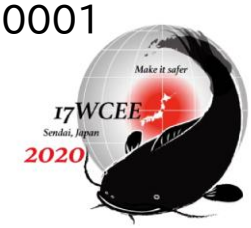

1. Introduction

Earthquakes can activate a number of geotechnical failures, such as liquefaction, loose deposits collapse, landslides, rock fall, rock avalanches, and landslide dams. Among these effects, soil and rock landslides are highly damaging [1]; thus, this study focusses on earthquake-triggered landslides.

The stability of slopes subject to earthquakes can be evaluated in several ways. The simplest approach is the pseudo-static analysis proposed in [2]. Such strategy consists basically in generalizing the classical static limit equilibrium method to the dynamic case; the stability of the most critical soil volume is checked by assuming that the seismic acceleration is represented by a static force. That force is related to the earthquake acceleration; some works propose to consider the maximum acceleration, others the average one, and others a given percentage of the maximum one [3]. In the pseudo-static analysis, the soil is assumed to be rigid; as a result, this formulation tends to be conservative [4-5]. In fact, many slopes experienced earthquake accelerations well above the yield threshold but suffered little or no permanent displacement [6]. Conversely, as this approach is highly inaccurate, the analyzed slopes could be unstable even if the safety factor is greater than 1 [2]. Another limitation of this strategy approach is the lack of any provided information on permanent displacements.

Complex finite element analyses can be used instead, but are not particularly well suited to reproduce landslides, given that such phenomena are highly complex, involving important discontinuities (i.e. slide displacement) and soil nonlinear behavior. Regarding the slide displacement, it can be reproduced with virtual highly flexible contact materials undergoing large strains, but most of the available software codes in geotechnical engineering do not consider large strains. Recent works try to overcome this difficulty by extending the original formulations or proposing meshless methods [7-9]. Concerning the nonlinear behavior, can be adequately reproduced, but an important number of soil parameters is required. Another difficulty is the necessity to consider absorbing boundary conditions in the analyzed soil domain; this is required to avoid unrealistic wave reflection. Moreover, the calculations involve an important number of operations, thus becoming impractical for day or mass use, as in Geographical Information Systems.

Given the above considerations, the Newmark method [10] was proposed as a simplified, although reliable, method to assess the seismic slope stability and to calculate its permanent displacement. The Newmark method analyzes, in a basic way, the dynamics of a rigid block sliding on a flat rough surface under earthquake shaking. Given its simplicity and reliability, the Newmark method has been widely used, both for research [11-12] and practical applications. Conversely, this strategy is oversimplified, and has not been fully calibrated with accurate nonlinear dynamic analyses, experimental results or observations from actual earthquakes; given this inaccuracy, the users themselves must judge the significance of the calculated displacement [12-13]. A number of improvements of the Newmark method have been proposed; the works [13-14] present detailed reviews. Some rather recent studies propose more accurate algorithms [15-20]. These strategies release most of the simplifications in the Newmark method; this work presents a formulation that tries to be accurate, reliable and general, while keeping most of the simplicity of the original Newmark approach. This research belongs a broader research initiative that involves testing and parametric analyses on actual situations.

2. Proposed formulation for seismic soil slope stability analysis

2.1. Introductory remarks

The proposed formulation is a simplified approach to estimate the slide displacement of a slope triggered by a known seismic acceleration. The sliding wedge is represented by a cubic block resting on an inclined flat surface. Two versions of the formulation are presented in the next two subsections; in 2.2 (more simplified) the block is considered infinitely rigid, and in 2.3 its flexibility is taken into consideration.

2.2. Formulation for rigid block

As discussed in subsection 2.1, the proposed formulation estimates the slide of a rigid block lying on a flat inclined surface parallel to the slope (soil surface). Figure 1.a shows such a situation, and Figure 1.b exhibits the actual sliding case (wedge) that the sketch in Figure 1.a is intended to represent (albeit only approximately).

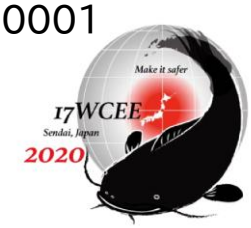

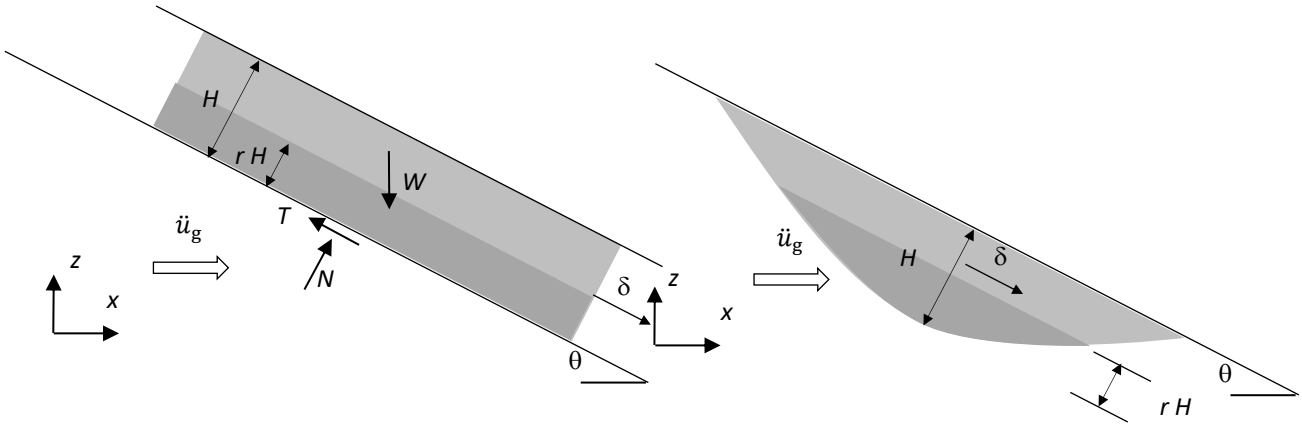

(a) Forces acting on the block (b) Actual situation to be represented

Figure 1. Rigid block sliding on a flat surface

Figure 1.a displays a block lying on an inclined plane with angle θ. In Figure 1.a, *W* and *H* represent the weight and height of the block, and *T* and *N* are the parallel (shear) and orthogonal (normal) reaction forces, respectively. The lower (darker) part of the block is below the water table; *r* is a dimensionless coefficient (ranging between 0 and 1) characterizing the water table position. The absolute parallel block displacement is denoted as δ, and $\ddot{u}_g$ is the horizontal seismic ground acceleration at the base (excitation). The two other components of the ground motion (vertical and horizontal inside the sliding plane) are not relevant, given that their influence on the block sliding is only moderate [21]. Noticeably, Figure 1 shows that only negative values of seismic acceleration are able to trigger a downward slide.

There are two possible conditions in the contact surface: stick (the relative displacement between the block and the base, $\delta - u_g \cos\theta$, is constant) and slip ($\delta - u_g \cos\theta$ is not constant). Under stick condition, the equations of motion of the block in the parallel and orthogonal directions are given by

$$W \sin\theta - T = \frac{W}{g}\ddot{u}_g \cos\theta \qquad W \cos\theta - N = -\frac{W}{g}\ddot{u}_g \sin\theta \tag{1}$$

If there is no water pressure (i.e. $r = 0$) or there is drained condition, the stick and slip conditions are defined by the Mohr-Coulomb criterion:

$$|T| \le c'\frac{W}{\gamma H} + N\left(1 - r\frac{\gamma_w}{\gamma}\right)\tan\phi' = c'\frac{W}{\gamma H} + \mu N\left(1 - r\frac{\gamma_w}{\gamma}\right) \tag{2}$$

In equation (2), γ and γ_w refer to the soil and water unit weight, and *c*' and ϕ' are the effective soil cohesion and friction angle, respectively; μ is the friction coefficient (μ = tan ϕ'). Noticeably, the cohesion term ($c'\frac{W}{\gamma H}$) should be only considered prior to the first slide; therefore, this contribution is commonly ignored in practical calculations.

If $r \neq 0$ (water pressure) and there is undrained condition, the stick and slip conditions are defined by:

$$|T| \le S_u\frac{W}{\gamma H} \tag{3}$$

In equation (3), S_u is the undrained strength; it behaves similarly to the cohesion, although it should not be considered only for the first slide but for the whole duration of the analysis. It should be kept in mind that S_u might change during the seismic action.

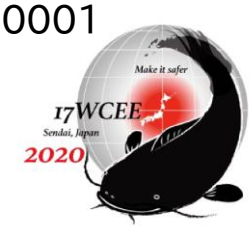

Under slip conditions, the block equation of motion in the parallel direction should be modified; conversely, the equation in the orthogonal direction remains unaltered. Thus, for drained and undrained conditions, the left equation (1) becomes, respectively:

$$W \sin\theta \pm \mu N\left(1 - r\frac{\gamma_w}{\gamma}\right) = \frac{W}{g}\ddot{\delta} \qquad W \sin\theta \pm S_u\frac{W}{\gamma H} = \frac{W}{g}\ddot{\delta} \tag{4}$$

The right equation (1) remains unaltered; can be used to obtain *N*.

In equation (4), the plus-minus sign arises from the fact that $\mu N\left(1 - r\frac{\gamma_w}{\gamma}\right)$ or $S_u\frac{W}{\gamma H}$ is opposed to the relative velocity between the block and the ground; obviously, the positive and negative signs correspond to shear force going downhill and uphill, respectively.

After equations (2) and (3), the stick-slip conditions are governed by the following conditions:

- The analysis starts with stick condition; the first slide begins once the shear demand reaches the shear strength: $|T| = \mu N\left(1 - r\frac{\gamma_w}{\gamma}\right)$ or $|T| = S_u\frac{W}{\gamma H}$.
- Stick resumes when the relative velocity drops to zero ($\dot{\delta} = \dot{u}_g \cos\theta$) and the shear demand is less than the shear strength ($|T| < \mu N\left(1 - r\frac{\gamma_w}{\gamma}\right)$ or $|T| < S_u\frac{W}{\gamma H}$).
- Slip starts again when $|T| = \mu N\left(1 - r\frac{\gamma_w}{\gamma}\right)$ or $|T| = S_u\frac{W}{\gamma H}$.

By replacing the shear strength conditions ($|T| = c'\frac{W}{\gamma H} + \mu N\left(1 - r\frac{\gamma_w}{\gamma}\right)$ or $|T| = S_u\frac{W}{\gamma H}$) in the equations of motion (1), the following critical values of the driving input acceleration are obtained:

$$\ddot{u}_g = \pm g\,\frac{\frac{c'}{\gamma H\cos\theta} + \left(1 - r\frac{\gamma_w}{\gamma}\right)\tan\phi' \mp \tan\theta}{1 \pm \tan\phi'\tan\theta} \qquad \ddot{u}_g = \pm g\left(\frac{S_u}{\gamma H\cos\theta} \mp \tan\theta\right) \tag{5}$$

Left equation (5) shows that the water pressure eases sliding, given that the effective stress term is reduced when $r \neq 0$.

Noticeably, by neglecting the contribution of the cohesion term and assuming that $r = 0$ (i.e. there is no water effect), the left condition in equation (5) becomes

$$\ddot{u}_g = \pm g\tan(\phi \pm \theta) \tag{6}$$

The original Newmark method [5,10] is a highly simplified approach to estimate the slide of a rigid block lying on a flat inclined surface (Figure 1.a). Apart from the simplifications in the previous development, the Newmark method does not contemplate the influence of water ($r = 0$) and considers other assumptions:

- Under slip condition, the block sliding displacement is obtained by integrating two times the part of input acceleration that exceeds the critical level (i.e. the difference between the seismic acceleration and such level: $\ddot{u}_g \mp g\tan(\phi \pm \theta)$). This situation involves a relevant simplifying condition given that equation (4) shows that the actual situation is different.
- Only downward slip motion is considered; in practice this assumption is equivalent to remove the absolute sign in equation (2), and to take only the negative sign in equation (4). In this situation, left equation (5) becomes $\ddot{u}_g = -g\,\frac{\frac{c'}{\gamma H\cos\theta} + \left(1 - r\frac{\gamma_w}{\gamma}\right)\tan\phi' + \tan\theta}{1 - \tan\phi'\tan\theta}$ and equation (6) turns into $\ddot{u}_g = -g\tan(\phi - \theta)$.

Noticeably, the results of Newmark method do not depend on the parallel extension of the block; this condition holds for the proposed strategy.

The Newmark method has become very popular, given its simplicity; however, it involves several relevant simplifying assumptions that might impair its accuracy and reliability. By summing up the above description,

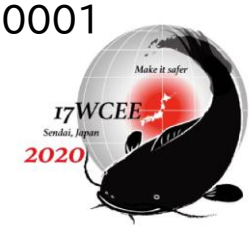

such suppositions are: (i) the slide of any soil volume is represented by the one of a cubic block (difference between Figure 1.a and Figure 1.b), (ii) the sliding block is infinitely rigid, (iii) the shear strength of soil is represented by a classical Mohr-Coulomb model, (iv) the upslope sliding resistance is infinitely large, as upslope sliding is not considered, (v) during sliding, the relative displacement between the block and the soil is described by double time integration of the portion of the seismic driving acceleration that exceeds the critical value, and (vi) the numerical integrations can be performed without special care to the numerical instability and inaccuracy. The proposed formulation releases the assumptions ii, iii, iv, v and vi.

2.3. Formulation for flexible block

As discussed previously, this subsection describes a more exact formulation accounting for the block flexibility. Figure 2 displays, similarly to Figure 1.a, the sliding block; Figure 2.a presents the discretization of the block with a lumped masses model, and Figure 2.b depicts the corresponding mechanical model. The bottom degree of freedom is denoted with "*b*", accounting for "base". The absolute parallel displacement of the base is represented by δ_b, and the relative parallel displacement of the *i*-th degree of freedom respect to the base is termed as d_i. In Figure 2.b, m_i, k_i and c_i refer to the mass, stiffness and damping associated to the *i*-th degree of freedom, respectively.

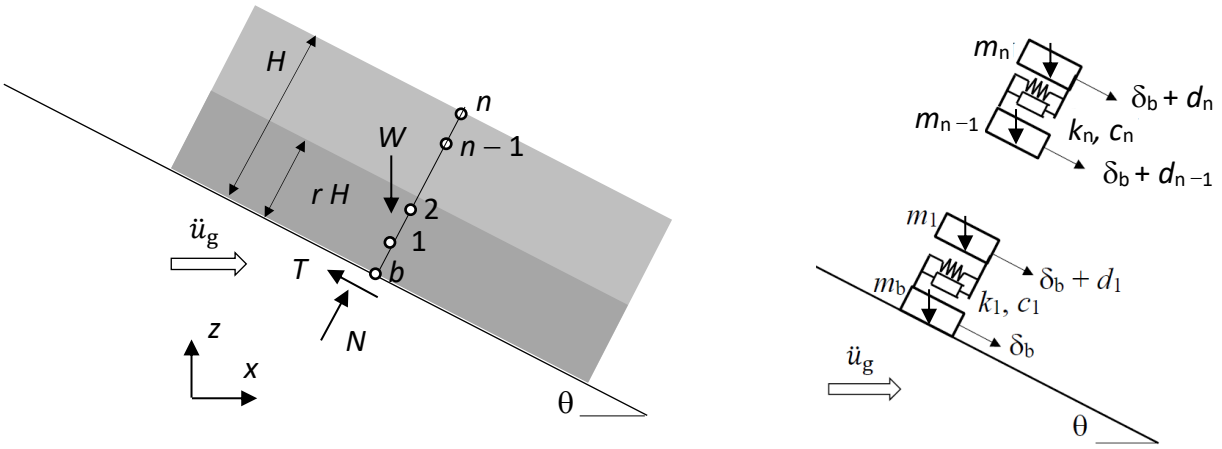

(a) Flexible block modelling (b) Lumped masses model

Figure 2. Flexible block sliding on a flat surface

Under **stick** condition ($\delta_b - u_g \cos\theta$ is constant), the motion of each lumped mass in the parallel direction is described by the following matrix equation:

$$\mathbf{M}\,\ddot{\mathbf{d}} + \mathbf{C}\,\dot{\mathbf{d}} + \mathbf{K}\,\mathbf{d} = -\mathbf{M}\,\mathbf{1}\left(\ddot{u}_g \cos\theta - g\ \sin\theta\right) \tag{7}$$

In equation (7), **d** is a vector that contains the parallel displacements of each DOF relative to the base (*b*), **M** and **K** are the mass and stiffness matrices, and **1** is the constant unit vector:

$$\mathbf{d} = \begin{pmatrix} d_1 \\ \vdots \\ d_n \end{pmatrix} \quad \mathbf{M} = \begin{pmatrix} m_1 & \cdots & 0 \\ \vdots & \ddots & \vdots \\ 0 & \cdots & m_n \end{pmatrix} \quad \mathbf{K} = \begin{pmatrix} k_1 + k_2 & -k_2 & 0 & & \\ -k_2 & k_2 + k_3 & -k_3 & & \\ 0 & -k_3 & k_3 + k_4 & & \\ & & & \ddots & \\ & & & k_{n-1} + k_n & -k_n \\ & & & -k_n & k_n \end{pmatrix} \quad \mathbf{1} = \begin{pmatrix} 1 \\ \vdots \\ 1 \end{pmatrix} \tag{8}$$

The damping matrix **C** can be generated by a Rayleigh model as $\mathbf{C} = \alpha\,\mathbf{M} + \beta\,\mathbf{K}$.

In the orthogonal direction, it is assumed that the block is infinitely rigid; then, both under stick and slip conditions, the motion is described (analogously to the second equation in (1)) by the following scalar equation:

$$g\ \mathbf{1^T M 1}\ \cos\theta - N = -\mathbf{1^T M 1}\ \ddot{u}_g\ \sin\theta \tag{9}$$

In the sliding surface, the base shear force (similarly to the first equation in (1)) is given by

$$T = -\mathbf{1^T M}\ \ddot{\mathbf{d}} - \mathbf{1^T M 1}\ (\ddot{u}_g \cos\theta - g\ \sin\theta) \tag{10}$$

Like in equations (2) and (3), the stick and slip conditions under drained and undrained conditions are respectively defined by:

$$|T| \le c'\ \frac{\mathbf{1^T M 1}}{\gamma H} + N\ \tan\phi'\ \left(1 - r\frac{\gamma_w}{\gamma}\right) = c'\ \frac{\mathbf{1^T M 1}}{\gamma H} + \mu N\left(1 - r\frac{\gamma_w}{\gamma}\right) \qquad |T| \le S_u\ \frac{\mathbf{1^T M 1}}{\gamma H} \tag{11}$$

In the left equation (Mohr-Coulomb criterion), as discussed after equation (2), the cohesion term ($c'\ \frac{\mathbf{1^T M 1}}{\gamma H}$) should be only considered prior to the first slide; thus, it is commonly neglected.

Under **slip** condition, a new DOF must be considered, given that the parallel motion of the base is not equal to that of the soil: $\delta_b \neq u_g \cos\theta$. In drained condition, the corresponding $n + 1$ equations of motion are

$$\begin{gathered}\mu N\left(1 - r\frac{\gamma_w}{\gamma}\right) = -(m_b + \mathbf{1^T M 1})\ (\ddot{\delta}_b - g\ \sin\theta) - \mathbf{1^T M}\ \ddot{\mathbf{d}} \\ \mathbf{M}\ \ddot{\mathbf{d}} + \mathbf{C}\ \dot{\mathbf{d}} + \mathbf{K}\ \mathbf{d} = -\mathbf{M 1}\ (\ddot{\delta}_b - g\ \sin\theta)\end{gathered} \tag{12}$$

The first (scalar) equation (12) is obtained by adding the $n + 1$ equations in (12); the second (matrix) equation correspond to the last n equations in (7).

In undrained condition, equations (12) become:

$$\begin{gathered}S_u\ \frac{\mathbf{1^T M 1}}{\gamma H} = -(m_b + \mathbf{1^T M 1})\ (\ddot{\delta}_b - g\ \sin\theta) - \mathbf{1^T M}\ \ddot{\mathbf{d}} \\ \mathbf{M}\ \ddot{\mathbf{d}} + \mathbf{C}\ \dot{\mathbf{d}} + \mathbf{K}\ \mathbf{d} = -\mathbf{M 1}\ (\ddot{\delta}_b - g\ \sin\theta)\end{gathered} \tag{13}$$

Equations (12) or (13) are solved by eliminating $\ddot{\delta}_b$; this leads to $\mathbf{M}^*\ \ddot{\mathbf{d}} + \mathbf{C}\ \dot{\mathbf{d}} + \mathbf{K}\ \mathbf{d} = \mathbf{M 1}\ \frac{\mu N\left(1 - r\frac{\gamma_w}{\gamma}\right)}{m_b + \mathbf{1^T M 1}}$ or $\mathbf{M}^*\ \ddot{\mathbf{d}} + \mathbf{C}\ \dot{\mathbf{d}} + \mathbf{K}\ \mathbf{d} = \mathbf{M 1}\ \frac{S_u\ \frac{\mathbf{1^T M 1}}{\gamma H}}{m_b + \mathbf{1^T M 1}}$, where $\mathbf{M}^* = \mathbf{M} - \frac{\mathbf{M 1 1^T M}}{m_b + \mathbf{1^T M 1}}$. Given that these equations have the same form that any standard linear matrix equation describing the motion of multi-degree of freedom systems (like (7)), all the available solution algorithms can be utilized. Once this equation is solved, the eliminated degree of freedom can be obtained by the first equation (12) or (13).

Alike to the criteria exposed after equation (2), the stick and slip conditions are governed by the following conditions:

- The first slide begins once the shear demand reaches the shear strength: $|T| = \mu\ N\left(1 - r\frac{\gamma_w}{\gamma}\right)$ or $|T| = S_u\ \frac{\mathbf{1^T M 1}}{\gamma H}$.
- Slip resumes when the relative velocity drops to zero ($\dot{\delta}_b = \dot{u}_g\ \cos\theta$) and the shear demand is less than the shear strength ($|T| < \mu\ N\left(1 - r\frac{\gamma_w}{\gamma}\right)$ or $|T| \le S_u\ \frac{\mathbf{1^T M 1}}{\gamma H}$).
- Slip starts again when $|T| = \mu\ N\left(1 - r\frac{\gamma_w}{\gamma}\right)$ or $|T| = S_u\ \frac{\mathbf{1^T M 1}}{\gamma H}$.

Conversely to the rigid case (subsection 2.2), these conditions do not lead to any constant critical acceleration (such as equations (5) and (6)). On the other hand, as discussed previously, the formulation in

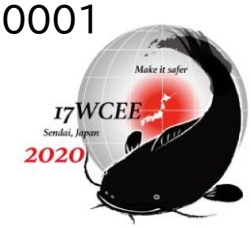

subsection 2.2 (rigid block) is independent on the parallel size of the block; this circumstance holds when the block flexibility is taken into consideration.

The presented approach extends the original Newmark method, but preserves the advantages of a relatively simple mathematical scheme. It can be considered as a "coupled" formulation, according to the general classification of strategies for calculating earthquake-triggered slope slide [13,22].

3. Numerical examples

3.1. General description

This section describes preliminary application examples of the proposed algorithm. The objective is to highlight its ability to reproduce the block sliding behavior, to point out the difference with the classical Newmark method, and to investigate the influence of the water and the block flexibility and damping in the sliding displacement. Subsection 3.2 presents an example on the earthquake-triggered sliding of a block resting on a flat surface, subsection 3.3 compares results from the proposed approach and the Newmark one, subsection 3.4 discusses the influence of the water pressure, and subsections 3.5 and 3.6 explore the influence of the soil (block) stiffness and damping parameters, respectively. Finally, subsection 3.7 discusses global remarks.

In all these examples, the driving ground motion is the FN (Fault Normal) Component of the Cholame-Shandon Array #5 record of the 17-08-1966 Parkfield earthquake; that event had moment magnitude 6.69. This input has 0.444 g maximum acceleration, 0.863 m/s Arias intensity [23], and 6.50 s effective duration [24]. The average shear wave velocity in the top 30 m is $v_{s,30}$ = 792 m/s; thus, the soil is classified as type B according to the American criteria [25].

3.2. Sliding of a rigid block on a flat surface

Figure 3 displays the results of the proposed algorithm by assuming that the block is infinitely rigid (subsection 2.2) and is sliding on a flat surface ($\theta = 0$). The block height is 8 m, and the main soil parameters are zero cohesion, unit weight 20 kN/m^3 and friction angle 5º; no water effect is considered. Figure 3 encompasses only the relevant (sliding) time interval.

Figure 3 shows a regular behavior, with expected results. Figure 3.a displays the forcing accelerogram and the two critical levels (equation (6)), and Figure 3.b presents the sliding displacement. Comparison among such plots shows that the stick and slip conditions described in subsection 2.2 are fulfilled; the final sliding displacement is – 45 mm; the negative sign indicates a leftward displacement.

3.3. Comparison between the Newmark and the proposed approaches

Figure 4 presents a comparison between the results of the proposed algorithm (assuming that the block is infinitely rigid, subsection 2.2) and the classical Newmark algorithm. The block height is 8 m, the slope angle is 15º and the main soil parameters are zero cohesion, unit weight 20 kN/m^3 and friction angle 25º; there is no water effect. Similarly to Figure 3, Figure 4 includes only the time interval where the sliding is concentrated.

Figure 4.a displays the driving seismic acceleration and the critical level given by equation (6) with negative sign: $\ddot{u}_g = -\,g\tan(\phi - \theta) = -\,0.176\,g$. Conversely, the level with positive sign ($\ddot{u}_g = g\tan(\phi + \theta) = 0.839\,g$) is never exceeded, thus showing that upslope slide never occurs. Figure 4.b shows that the difference between the proposed formulation and the classical Newmark method is significant, being on the unsafe side. In this example, the final sliding displacement according to the Newmark and the proposed strategies are 12.2 and 13.9 mm, respectively (almost 14% increment).

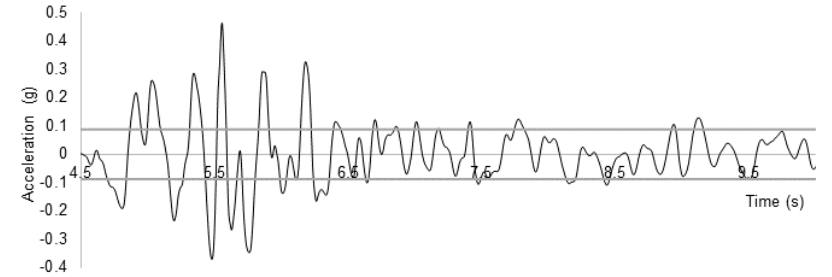

(a) Driving ground motion ($\ddot{u}_g$)

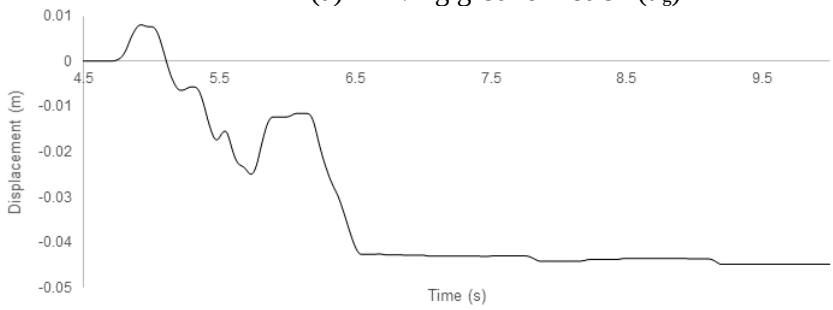

(b) Sliding relative displacement ($\delta - u_g$)

Figure 3. Results from the proposed formulation. Rigid block, H = 8 m, θ = 0, γ = 20 kN/m^3, c = 0, ϕ = 5º, r = 0

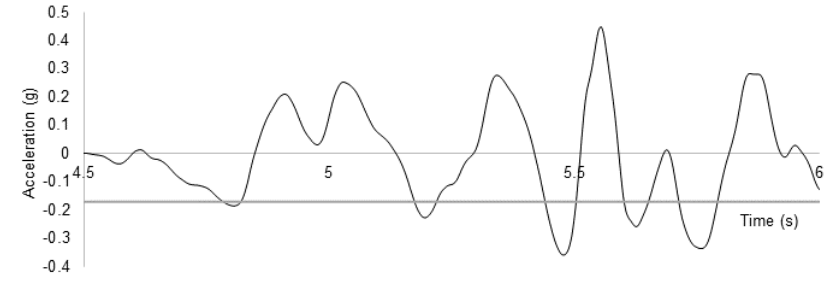

(a) Parallel component of the driving ground motion ($\ddot{u}_g \cos\theta$)

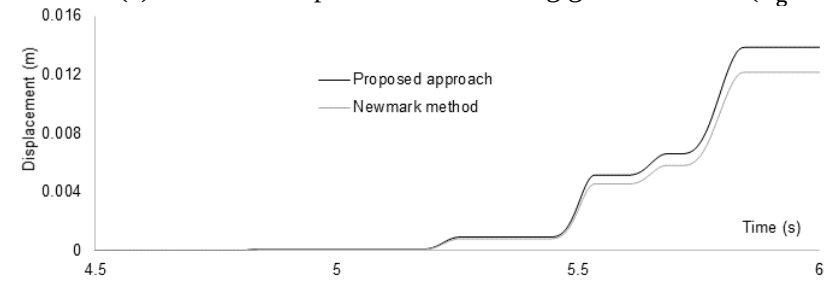

(b) Sliding displacement ($\delta - u_g \cos\theta$)

Figure 4. Comparison between the Newmark and the proposed formulation. Rigid block, H = 8 m, θ = 15º, γ = 20 kN/m^3, c = 0, ϕ = 25º, r = 0

3.4. Influence of water

Figure 5 describes the results provided for the proposed algorithm in the same case considered in Figure 4, except for the presence of water pressure; the following values of r (Figure 1) are considered: 0, 0.1, 0.2, 0.3 and 0.4. The Mohr-Coulomb criterion is used to describe the sliding condition (equation (2)).

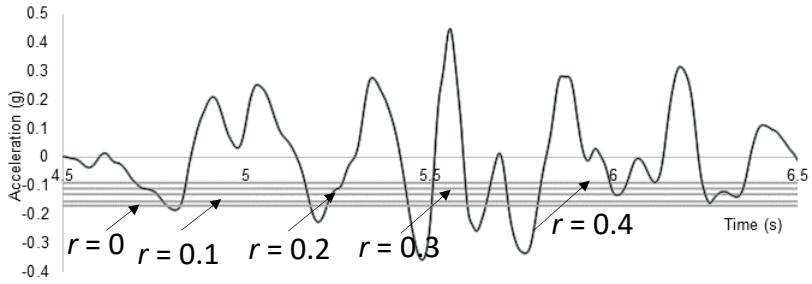

(a) Parallel component of the driving ground motion ($\ddot{u}_g \cos\theta$)

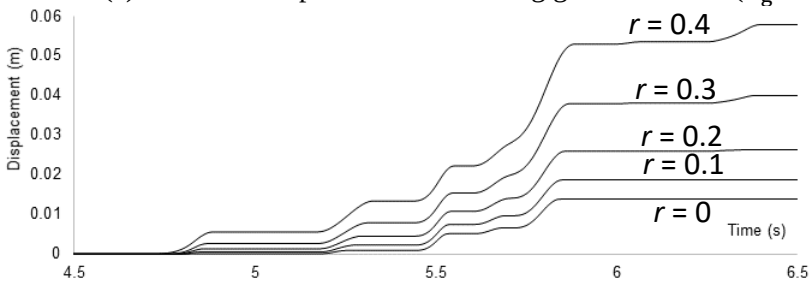

(b) Sliding displacement ($\delta - u_g \cos\theta$)

Figure 5. Influence of the water pressure with drained condition (Mohr-Coulomb criterion). Rigid block, H = 8 m, θ = 15°, γ = 20 kN/m^3, c = 0, ϕ = 25°, r = 0, 0.1, 0.2, 0.3, 0.4

Figure 5.a displays the seismic acceleration and the critical level, as provided by equation (6) (with negative sign); such level decreases with increasing r, thus showing that the water pressure facilitates sliding. This trend is confirmed by Figure 5.b; the final sliding displacement is 13.8 mm (r = 0), 18.7 mm (r = 0.1), 26.3 mm (r = 0.2), 40.0 mm (r = 0.3) and 57.9 mm (r = 0.4).

Figure 6 presents a comparison between the drained and undrained conditions, equations (2) and (3), respectively. The considered situation is similar to the one in Figure 5 with r = 0.4; for the undrained condition, S_u = 150 kPa is adopted.

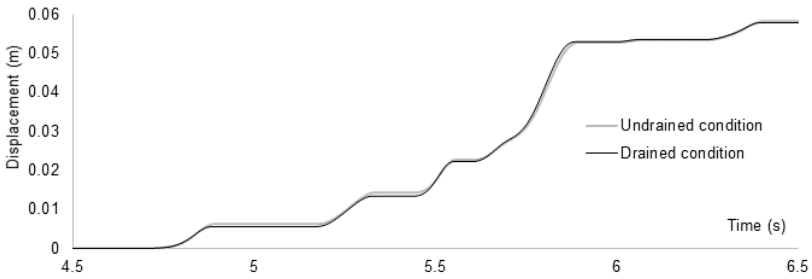

Figure 6. Comparison between the results for drained and undrained conditions. Rigid block, H = 8 m, θ = 15°, γ = 20 kN/m^3, r = 0.4

Figure 6 highlights the ability of the proposed algorithm to simulate the involved phenomena.

3.5. Influence of the block flexibility

This subsection presents an application of the formulation for flexible block described in subsection 2.3. As discussed in subsection 3.1, the average shear wave velocity in the top 30 m is $v_{s,30}$ = 290 m/s; therefore, given that the soil unit mass is ρ = 2000 kg/m^3, the shear modulus is G = 290^2 × 2000 = 168.2 MPa ($v_s = \sqrt{G/\rho}$). Then, by assuming that the Poisson ratio is ν = 0.3, the elastic modulus is E = 168.2 × 2 × 1.3 = 437.32 MPa ($E = G\,2\,(1+\nu)$). Given that the results of the analysis do not depend on the block dimensions in the parallel direction, a unit area (1 m^2) is considered; then, the soil is discretized with 17 degrees of freedom (b-16, Figure

2.a), thus, n = 16. The masses associated to each node are $m_b = m_{16}$ = 500 kg and $m_1 = \ldots = m_{15}$ = 1000 kg. Given that the height of each discrete layer is 8 / 16 = 0.5 m (Figure 2.b), the stiffness coefficients are equal to k_i = 168.2 N/mm^2 × 1 m^2 / 0.5 m = 3.364 × 10^8 N/m (i = 1–16). The damping matrix is generated after a Rayleigh model by imposing that in the 1st and 3rd modes there is a 5% damping ratio; the values of the combination coefficients are α = 1.50 s^{-1} and β = 9.34 10^{-4} s. The obtained damping ratios for the 2nd and 4th modes are 0.039 and 0.064, respectively; this shows an adequate compensation.

After these mass and stiffness values, a linear eigenvalue (modal) analysis is performed. The first eigenvalue is ω_1 = 56.90 rad/s, corresponding to a soil fundamental period T_F = 0.1104 s; this value is highly close to the classical approximation [5] given by $T_F = 4\,H / v_s = 4 \times 8 / 290 = 0.110$ s. This coincidence confirms the accuracy and reliability of the considered model. Another relevant output of this modal analysis is that the first mode mass participation factor is 81.81%; this highlights the feasibility of representing the block by this (fundamental) mode.

Figure 7 presents a comparison between the results provided by the two versions of the proposed algorithm: assuming that the sliding block is infinitely rigid (subsection 2.2), and taking into consideration the block flexibility (subsection 2.3). The analyzed case is the same than in Figure 4.

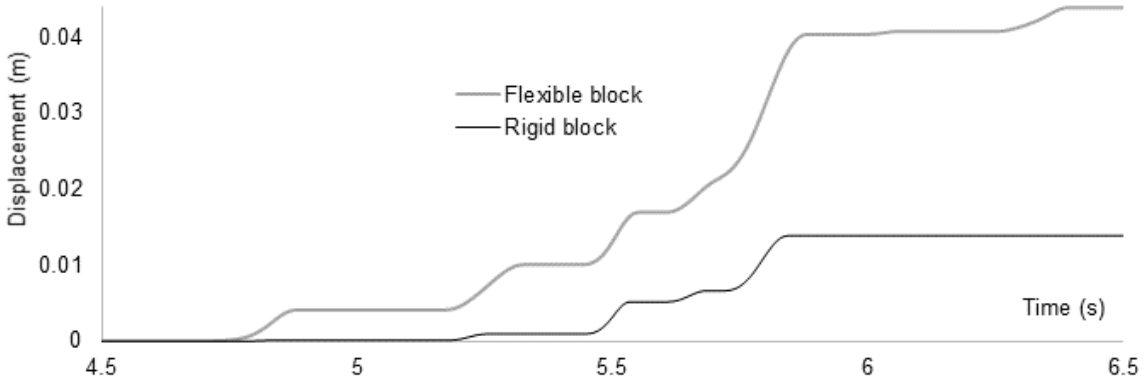

Figure 7. Comparison between the results for rigid and flexible block. H = 8 m, θ = 15º, γ = 20 kN/m^3, c = 0, ϕ = 25º, r = 0

Figure 7 shows that the influence of the soil (block) flexibility is high. The sliding displacement obtained by assuming that the block is infinitely rigid is 13.8 mm (Figure 4), while the consideration of the block flexibility yields 43.9 mm.

To further emphasize the accuracy and reliability of the proposed model, additional calculations are performed; such analyses correspond to intermediate values of the soil stiffness ranging between the actual value (E = 437.32 MPa) and infinite (rigid block, subsection 2.2). When the deformation modulus is multiplied by 10, 100, 1000, 10000 and 100000, the obtained displacements are 31.1 mm, 19.9 mm, 15.3 mm, 14.3 mm, and 13.8 mm, respectively. These results show that the calculated displacements tend to approach the value for $E = \infty$ (13.8 mm).

3.6. Influence of the block damping

This subsection discusses the influence of the soil (block) damping in the sliding behavior. Figure 8 displays, for the same case discussed in subsection 3.5, results for different values of the damping ratio. Noticeably, the three considered values (0.03, 0.05 and 0.10) cover the most feasible situations for actual soils possessing the characteristics of the considered one (shear wave velocity equal to 290 m/s); in fact, the highest value would correspond to severe damaged condition.

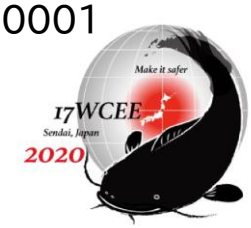

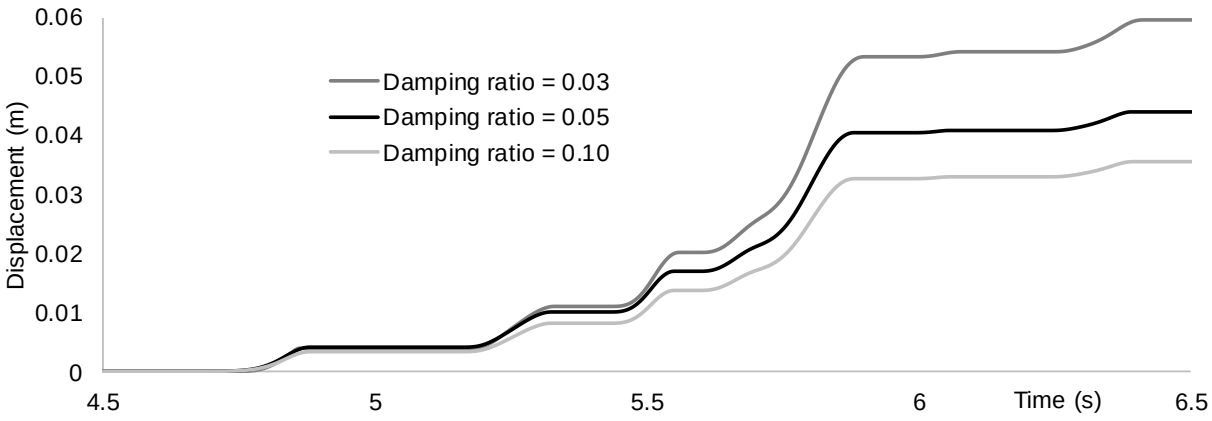

Figure 8. Influence of the block damping. E = 437.32 MPa, H = 8 m, θ = 15º, γ = 20 kN/m^3, c = 0, ϕ = 25º, r = 0

Figure 8 shows that the influence of damping is significant. More precisely, the more damping, the less sliding displacement; this circumstance can be explained by the near-constancy of the input energy.

3.7. Global remarks

The results presented in the previous subsections point out that the proposed algorithm is capable to reproduce the block sliding behavior in the conditions discussed in its formulation (subsection 2). Whenever possible, the observed trends are interpreted in light of the expected behavior.

4. Conclusions

This paper presents a computationally efficient formulation to calculate the permanent displacement of flexible soil blocks resting on inclined rough surfaces and undergoing horizontal seismic shaking; noticeably, the influence of the water pressure is contemplated. The sliding criteria consider both drained (Mohr-Coulomb) and undrained conditions. A number of simulations are presented; they are selected to show the capability of the algorithm to reproduce all the considered issues, and to highlight its accuracy and reliability. All the obtained results are satisfactory; the procedure can be used to assess the safety conditions of slopes during earthquakes albeit keeping a low computational effort.

Further research includes conducting parametric studies on actual slope situations, performing landslide experiments, and improving the capabilities of the proposed algorithm; such advances are oriented to consider the soil nonlinear behavior and to release the assumption of a specified (imposed) sliding surface. This last objective can be attained by checking the stick/slip condition at each node and time instant.

5. Acknowledgements

This work has received financial support from the State Key Laboratory of Geohazard Prevention and Geoenvironment Protection of the Chengdu University of Technology Open Fund (Grant No. SKLGP2019K010). As well the Spanish Government (MINECO, projects BIA2017-88814-R and CGL2015-6591) and the European Commission (FEDER) have provided funds. The stay of Ms. Dong in Barcelona was funded by the Sichuan Provincial Youth Science and Technology Innovation Team Special Projects of China (Grant No. 2017TD0018). Key scientific and technological projects of transportation industry in 2018 (2018-ZD5-029). These supports are gratefully acknowledged.

6. References

[1] Kobayashi Y. (1981). Causes of fatalities in recent earthquakes in Japan. *Journal of Disaster Science*, **3**:15–22.

[2] Terzaghi K. (1950). Mechanisms of landslides. *Engineering Geology. Geological Society of America*.

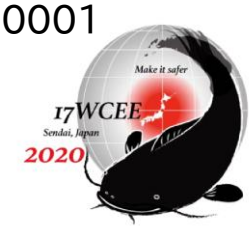

[3] Tan D. (2006). Seismic slope safety – Determination of critical slip surface using acceptability criteria. *Doctoral Thesis. Imperial College, London*.

[4] Seed HB. (1979). Considerations in the earthquake-resistant design of earth and rockfill dams. *Geotechnique*, **29**(3):215-263.

[5] Kramer SL. (1996). Geotechnical Earthquake Engineering. *Prentice-Hall*.

[6] Wilson RC, Keefer DK. (1983). Dynamic Analysis of a Slope Failure from the 6 August 1979 Coyote Lake, California Earthquake. *Bulletin of the Seismological Society of America*, **73**(3):863-877.

[7] Di Y, Sato T. (2004). A practical numerical method for large strain liquefaction analysis of saturated soils. *Soil Dynamics and Earthquake Engineering*, **24**(3):251-260.

[8] Blanc T, Pastor M. (2013). A stabilized Smoothed Particle Hydrodynamics, Taylor-Galerkin algorithm for soil dynamics problems. *International Journal for Numerical and Analytical Methods in Geomechanics*, **37**(1):1-30.

[9] Soga K, Alonso E, Yerro A, Kumar K, Bandara S. (2016). Trends in large-deformation analysis of landslide mass movements with the particular emphasis on the material point method. *Géotechnique* **66**(3):248-273.

[10] Newmark NM. (1965). Effects of earthquakes on dams and embankments. *Geotechnique*, **15**(2):139:160.

[11] Garini E, Gazetas G, Anastasopoulos I. (2011). Asymmetric 'Newmark' sliding caused by motions containing severe 'directivity' and 'fling' pulses. *Géotechnique*, **61**(9):733-756.

[12] Jibson RW. (2007). Regression models for estimating coseismic landslide displacement. *Engineering Geology,* **91**(2), 209-218.

[13] Jibson RW. (2011). Methods for assessing the stability of slopes during earthquakes—A retrospective. Engineering *Geology* **122**:43–50.

[14] Rathje EM, Bray JD. (1999). An Examination of Simplified Earthquake-induced Displacement Procedures for Earth Structures. *Canadian Geotechnical Journal*, **36**:72-87.

[15] Romeo R. (2000). Seismically induced landslide displacements: a predictive model. *Engineering Geology*, **58**(3):337-351.

[16] Bray JD, Travasarou T. (2009). Pseudostatic Coefficient for Use in Simplified Seismic Slope Stability Evaluation. *Journal of Geotechnical and Geoenvironmental Engineering*, **135**(9):1336-1340.

[17] Baziar MH, Rezaeipour H, Jafarian Y. (2012). Decoupled Solution for Seismic Permanent Displacement of Earth Slopes Using Deformation-Dependent Yield Acceleration. *Journal of Earthquake Engineering*, **16**:917–936.

[18] Brun M, Gravouila A, Combescurea A, Limam A. (2015). Two FETI-based heterogeneous time step coupling methods for Newmark and α-schemes derived from the energy method. *Computer Methods in Applied Mechanics and Engineering*, **283**:130-176.

[19] Lashgari A, Jafarian Y, Haddad A. (2018). Predictive model for seismic sliding displacement of slopes based on a coupled stick-slip-rotation approach. *Engineering Geology*, **244**:25-40.

[20] Cattoni E, Salciarini D, Tamagnini C. (2019). A Generalized Newmark Method for the assessment of permanent displacements of flexible retaining structures under seismic loading conditions. *Soil Dynamics & Earthquake Engineering*, **117**:221-233.

[21] Du W. (2018). Effects of directionality and vertical component of ground motions on seismic slope displacements in Newmark sliding-block analysis. *Engineering Geology*, **239**:13-21.

[22] Rathje EM, Bray JD. (2000). Nonlinear Coupled Seismic Sliding Analysis of Earth Structures. *Journal of Geotechnical and Geoenvironmental Engineering*, **126**(11):1002-1013.

[23] Arias A. (1970). A measure of earthquake intensity. Seismic Design for Nuclear Power Plants. *MIT Press* 438-443.

[24] Trifunac MD, Brady AG. (1975). Study on the duration of strong earthquake ground motion. *Bulletin of the Seismological Society of America* **65**(3):581–626.

[25] ASCE 7–16 (2016). Minimum design loads and associated criteria for buildings and other structures, American *Society of Civil Engineers*.

